Sensor Fusion for Cooperative Perception using Distance-weighted Dempster's Rule of Combination

Sumiko Miyata
Institute of Science Tokyo
Tokyo, Japan
sumiko@ict.eng.isct.ac.jp

Takamichi Miyata
Chiba Institute of Technology
Chiba, Japan
takamichi.miyata@it-chiba.ac.jp

Yasir Ali
Loughborough University
Loughborough, UK
y.y.ali@lboro.ac.uk

Ashleigh Filtness
Loughborough University
Loughborough, UK
A.J.Filtness@lboro.ac.uk

***Abstract*—Many traffic collisions at urban intersections are caused by human misperception and delayed judgment. V2X (vehicle-to-everything) cooperative perception mitigates this limitation by enabling vehicles equipped with cameras and roadside units (RSUs) to share information about objects outside the driver's field of view. Practical deployment requires incentives for data sharing and sensor fusion that reliably integrates uncertain observations. Our focus is on fusion using Dempster's rule of combination from Dempster–Shafer evidence theory, which can explicitly represent an unknown state and is therefore well suited to occupancy grid maps with occlusions. However, conventional fusion does not account for distance-dependent degradation and may place too much trust in distant sensors. We propose a distance-weighted combination rule on an occupancy grid map and introduce a hybrid scheme to limit computational cost. Numerical experiments in an urban intersection scenario suggest reduced false alarms and missed detections, thereby improving occupancy reliability without significantly increasing processing time.**

***Index Terms*—Sensor Fusion, Autonomous Driving Maps, Dempster's Rule of Combination**

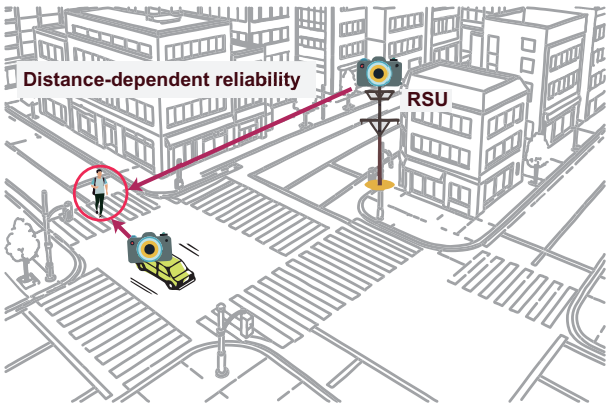

Fig. 1: Distance-weighted Dempster-Shafer sensor fusion for object detection at an intersection. This accounts for distance uncertainty, resulting in a more accurate belief.

I. Introduction

Many traffic accidents are caused by "human factors" such as misperception and delayed judgment. In particular, at urban intersections where pedestrians and vehicles interact in complex ways, the limits of human perception and blind spots created by buildings or large vehicles can cause hazardous objects to suddenly appear from outside the driver's field of view, leading to serious collisions. To technically compensate for such human errors and improve traffic safety at intersections, it is important to deploy V2X (Vehicle-to-Everything) cooperative perception systems in which vehicles share information with roadside units (RSUs) and other vehicles, thereby providing environmental information that cannot be obtained by a single vehicle alone [1]–[3].

The authors have previously proposed a Shapley-value-based fair incentive mechanism to establish cooperative perception as a sustainable social infrastructure [4]. In this framework, diverse stakeholders are encouraged to continuously provide data from cameras and LiDAR sensors, with the aim of maintaining a high-density sensing network and improving AI recognition accuracy over the long term. Building on that prior work, this paper advances the cooperative-perception pipeline by addressing the sensor-fusion layer—i.e., how the shared multi-sensor data should be integrated into a reliable occupancy grid map for safety-critical decision making. However, for safety-critical applications, data collection alone is insufficient; the fusion stage must suppress both false positives and false negatives when integrating observations from multiple sensors. If incorrect fusion leads to the detection of an object that does not actually exist, unnecessary alerts may induce "alert fatigue" in drivers, whereas missing a truly dangerous object may expose drivers, who trust the system, to collision risk without sufficient time to react.

As methods for integrating uncertain information from multiple sensors, approaches such as averaging, Bayesian inference, and Kalman filtering have been widely used, together with Dempster's rule of combination based on evidence theory [5], [6]. Evidence theory has the advantage that, in addition to "object present / object absent" for a grid cell, it can explicitly represent an "Unknown" state, which allows unobservable regions in an occupancy grid map to be modeled in a natural way. However, the conventional Dempster's Rule of Combination does not explicitly account for the degradation of detection accuracy caused by the distance between a sensor and a target object, and noisy evidence from distant sensors is fused with the same weight as evidence from nearby sensors. As a result, false detections from distant sensors may produce high confidence for objects that do not actually exist, while the existence probability of truly dangerous objects may be

unnecessarily suppressed.

In this paper, we propose a sensor fusion method based on a distance-weighted Dempster's rule of combination, in which the reliability of each sensor is weighted according to its geometric distance to the target grid cell as shown in Fig. 1. Moreover, we adopt a hybrid scheme in which the standard Dempster's rule of combination is used when the distance difference among sensors is small, and the distance-weighted rule is applied only when the distance difference is large, so that the increase in computational cost is kept small while reducing false positives and missed detections in distant grid.

The rest of the paper is organized as follows. Section II reviews related work and Dempster's rule. Section III presents the system setup and proposed fusion method. Section IV evaluates the baseline and proposed methods. Section V discusses the results in terms of intersection safety, and Section VI concludes.

II. Related work and preliminaries

A. Related work

In this section, we review related work on sensor fusion methods. Sensor fusion refers to the process of integrating information from multiple sensors to reduce false detections [7], [8]. A variety of fusion techniques have been proposed for this purpose. These include conventional methods such as simple averaging and least-squares estimation [9], as well as more advanced approaches based on Kalman filtering [10], [11], Bayesian theory [12], weighted averaging [13], [14], neural networks [15], and Dempster's rule of combination from evidence theory [16].

However, conventional approaches like simple averaging [9] often degrade detection accuracy when dealing with complex sensor data. While straightforward, these methods may fail to properly handle sensor uncertainties and inconsistencies. Kalman-filter-based methods [10], [11], on the other hand, require repeated execution of highly complex computations, which results in significant implementation costs. Furthermore, these methods are mainly used for self-localization tasks, making them less suitable for the objectives of the present study. Bayesian-theory-based approaches [12] can also present challenges. For instance, if a grid cell is mistakenly judged as occupied when no object actually exists, the occupancy probability of that cell can become excessively high. Although such errors may not directly compromise collision avoidance safety, they can lead to traffic congestion and adversely affect driving comfort.

In contrast, methods based on evidence theory offer a notable advantage by explicitly incorporating the uncertainty of "unknown object existence" within a grid cell. This allows non-detection cases to be considered in the fusion process, thereby improving overall detection accuracy [16].

In this paper, we adopt Dempster's rule of combination from evidence theory and further enhance it by incorporating the distance between sensors and objects into the fusion process. This extension aims to achieve even greater detection accuracy.

B. Dempster's Rule of Combination

Dempster's rule of combination provides a method for combining two basic probability assignments m_1 and m_2 to obtain a new assignment $\bar{m}$ [5], [6]. The combination is given by the following Eq. (1):

$$\bar{m}(A) = \frac{\sum_{B \cap C = A} m_1(B)\, m_2(C)}{1 - \sum_{B \cap C = \emptyset} m_1(B)\, m_2(C)} \tag{1}$$

Here, letting Θ denote the set of all possible states, A, B, C are subsets of Θ, and $m_1(B)$, $m_2(C)$ represent the basic probability masses assigned to subsets B and C by different information sources. The numerator sums the products $m_1(B)m_2(C)$ over all pairs satisfying $B \cap C = A$, and reflects the degree to which both information sources jointly support hypothesis A. Meanwhile, the denominator is $1 - k$, where k is the total mass assigned to mutually exclusive hypotheses and corresponds to the conflict between the two belief functions. Through this normalization, $\bar{m}(A)$ incorporates only the consistent evidence shared by the two sources, while discarding conflicting evidence.

Camarda et al. proposed a cooperative perception framework in which connected vehicles exchange evidential occupancy grids that are then fused using standard Dempster's rule, with discounting applied to account for pose uncertainty and information aging [17]. Ben Ayed et al. further surveyed evidential fusion for cooperative occupancy modeling and benchmarked various existing combination rules in simulation, but did not investigate distance-aware weighting of Dempster fusion [18]. While their method mainly addresses inter-vehicle alignment uncertainty, our approach focuses on distance-dependent sensing reliability and introduces distance-weighted Dempster fusion to suppress the influence of unreliable far-range observations.

III. Proposed method

A. Assumed System

In this study, we assume a V2X-based cooperative perception system in which multiple sensors deployed around an urban intersection share environmental information with roadside units (RSUs) and automated vehicles. Each sensor is either an on-board sensor mounted on a vehicle, such as a camera or LiDAR, or a roadside sensor installed on traffic signals or streetlights, and observes the monitoring area around the intersection from its known installation position. The monitoring area is discretized as an occupancy grid map, and each grid cell stores a probability vector over three states: Empty, Occupy, and Unknown.

For each grid cell within its sensing range, a sensor transmits to the RSU a probability vector whose elements represent the probability that no object is present (Empty), the probability that an object is present (Occupy), and the uncertainty caused by detection failure or occlusion (Unknown). The map-generation module running on the RSU or on an edge server computes the Euclidean distance d_i between sensor i and each target grid cell from the known sensor locations and grid coordinates, and

determines a reliability weight w_i for each sensor based on this distance.

When probability vectors from multiple sensors are available for the same grid cell, they are fused into a single probability vector using the proposed distance-weighted Dempster's Rule of Combination. The resulting occupancy grid map is then disseminated via V2X communication to vehicles passing through the intersection and is used to provide early warnings about pedestrians or other vehicles that are hidden in the driver's blind spots.

B. Sensor Information Fusion Based on Distance-weighted Dempster's Rule of Combination

In the previous subsection, we described the V2X-based cooperative perception system considered in this study and the structure of the probability vectors assigned to each grid cell. When the same grid cell is observed by multiple sensors, the probability vectors obtained from each sensor must be fused while reflecting the reliability of each sensor. In this subsection, based on Dempster's Rule of Combination introduced in Section II-B, we formulate an extended combination rule that incorporates weighting according to the distance between each sensor and the target grid cell.

Following Dempster's rule of combination, we combine two probability vectors $\mathbf{m}_1$ and $\mathbf{m}_2$ using distance-based reliability weights w_1 and w_2. The weights are inversely proportional to the distances d_1 and d_2 from sensor 1 and sensor 2 to the target grid cell, and are normalized so that their sum is equal to one, i.e., $w_1 + w_2 = 1$. They are defined as

$$w_i = \frac{1/d_i}{1/d_1 + 1/d_2}, \quad i = 1, 2.$$

We denote each probability vector $\mathbf{m}_i$ $(i \in \{1, 2\})$ as

$$\mathbf{m}_i = (m_{i,e},\, m_{i,o},\, m_{i,u}),$$

where the elements correspond to Empty, Occupy, and Unknown, respectively. For this vector, we define the elements of the distance-weighted probability vector $\mathbf{m}'_i = (m'_{i,e},\, m'_{i,o},\, m'_{i,u})$ as follows.

$$m'_{i,s} = \frac{m_{i,s}^{w_i}}{\sum_{t \in \{e,o,u\}} m_{i,t}^{w_i}},$$

where $s \in \{e, o, u\}$.

The degree of conflict (collision rate) k between the weighted probability vectors is defined as

$$k = m'_{1,e}\, m'_{2,o} + m'_{1,o}\, m'_{2,e}.$$

This quantity represents the amount of conflict between the mutually exclusive states "Empty" and "Occupy." To compensate for this conflict, we define the normalization coefficient α as

$$\alpha = \frac{1}{1 - k}.$$

Based on the distance-weighted Dempster–Shafer rule, the fused probabilities for the Empty, Occupy, and Unknown states are

$$\tilde{m}_e = \alpha\big(m'_{1,e}m'_{2,e} + m'_{1,e}m'_{2,u} + m'_{2,e}m'_{1,u}\big), \tag{2}$$

$$\tilde{m}_o = \alpha\big(m'_{1,o}m'_{2,o} + m'_{1,o}m'_{2,u} + m'_{2,o}m'_{1,u}\big), \tag{3}$$

$$\tilde{m}_u = \alpha\big(m'_{1,u}m'_{2,u}\big).$$

By applying the above distance-weighted Dempster's rule of combination, we obtain a new probability vector

$$\tilde{\mathbf{m}} = (\tilde{m}_e, \tilde{m}_o, \tilde{m}_u).$$

In this way, the outputs of multiple sensors for each grid cell can be fused into a single probability vector.

IV. Evaluation Experiment

A. Setting parameters

In this section, we evaluate the proposed sensor fusion method based on the distance-weighted Dempster's rule of combination (Proposed) from two perspectives: processing time and accuracy. As comparison methods, we use the conventional method (Conventional) and the baseline method (Baseline).

In this study, we use a square area with a side length of 500 m as the simulation domain. The area is discretized into 0.5 m $\times$ 0.5 m grid cells (1000×1000).

First, we generate ground-truth data for all grid cells. Each cell is assigned a value of 0 or 1, where a cell with value 0 is treated as "no object present," and a cell with value 1 is treated as "object present."

Next, we select the grid cells on which sensors are placed from the 1,000,000 cells. Each sensor can detect the grid cells within a circular area of radius 200,m, and the number of sensors is set to 16. This is because four sensors can cover the entire simulation area once, so with 16 sensors the entire area can be observed at least four times, which is expected to provide sufficient detection accuracy even for the conventional method.

Next, for each grid cell within the sensing range of a sensor, we assign probabilities corresponding to the three states: *Empty*, *Occupy*, and *Unknown*. These probabilities are determined with reference to the ground-truth data, and are configured so that the misdetection rate increases as the distance from the sensor becomes larger. Note that this evaluation does not aim to faithfully reproduce all real-world sensor errors; instead, we employ a simplified noise assumption that models uncertainty mainly as a function of the sensor–cell distance.

Here, let d_i denote the distance between sensor i and a grid cell, let the sensing radius of each sensor be $R = 200$ m, and let $\gamma \in \{6, 7, \ldots, 15\}$ be a parameter that controls the increase of misdetection with distance. If we denote by $\varepsilon(d_i; \gamma)$ the probability that a grid cell which is truly empty is incorrectly output as Occupy or Unknown, then in this simulation we model it, for simplicity, as a linear function that increases in proportion to the distance d_i,

$$\varepsilon(d_i; \gamma) = \varepsilon_0 + \frac{\gamma}{100}\frac{d_i}{R}.$$

Similarly, when the true state is Occupy, we assign the misdetection probability toward Empty also by $\varepsilon(d_i;\gamma)$, so that misdetections become more likely as the distance d_i increases and as the parameter γ becomes larger. Here, ε_0 represents the baseline misdetection rate at distance $d_i = 0$, and in this simulation it is set to $\varepsilon_0 = 0.0625$, corresponding to the Dirichlet parameter $(30, 1, 1)$. By varying this parameter, we can simulate a wide range of sensing conditions, from situations where data acquisition is easy (e.g., clear weather) to environments where it is difficult due to heavy fog or rain.

For grid cells whose sensing regions overlap across multiple sensors, the probability vectors obtained from each sensor are fused into a single probability vector using the distance-weighted Dempster's rule of combination proposed in Section III. Finally, a threshold is applied to the probability vector of each grid cell; if the probability of one of the states exceeds the threshold, that state is taken as the decision for the cell, and this decision is compared with the ground-truth data for accuracy evaluation.

B. Comparison Methods and Evaluation Conditions

In this subsection, we describe the methods used for comparison in this study and their evaluation conditions. The main parameter settings for each method are summarized in Table I. We consider three methods: the conventional method (Conventional), the baseline method (Baseline), and the proposed method (Proposed).

In the conventional method (Conventional), we assume 40 sensors representing on-vehicle LiDARs, and each sensor is randomly placed within the simulation area. In the baseline method (Baseline), the sensor fusion algorithm itself is the same as in the conventional method, namely the standard Dempster's rule of combination, but the number of sensors is fixed to 16 and their locations are also fixed. This ensures that all grid cells are observed at least once, and that four sensor fusion operations are performed for each grid cell.

In the proposed method (Proposed), the number and placement of sensors are identical to those of Baseline, and only the sensor fusion method is changed. Specifically, as formulated in Section III, the distance-weighted Dempster's rule of combination is used when the distance difference between sensors and the target grid cell is large, whereas the standard Dempster's rule of combination, as in Baseline, is used when the distance difference is small, resulting in a hybrid scheme.

Regarding the evaluation metrics, processing time is compared among the three methods: Conventional, Baseline, and Proposed. On the other hand, for accuracy evaluation, we compare only Baseline and Prop, and exclude the Conventional method. As described in the previous subsection, we prepare ground-truth data for all grid cells by simulation, and define the accuracy metric as the fraction of cells whose estimated state matches the ground truth. In contrast, the Conventional method assumes random sensor placement, and many grid cells remain unobserved; therefore, it is not designed for an evaluation scheme in which all grid cells are matched one-to-one with the ground truth to compute the accuracy. For this reason, it is difficult to apply the accuracy metric used in this paper fairly to the Conventional method, and the accuracy plots focus on the comparison between Baseline and Proposed.

C. Evaluation Metrics and Evaluation Strategy

In this subsection, we describe the evaluation metrics used in this study and the comparison strategy. We employ two metrics: processing time and accuracy.

For processing time, we define the processing time as the elapsed time from when all 16 sensors start their detection processing until probability vectors have been generated for all grid cells.

For accuracy, we use the agreement between the probability vectors stored in each grid cell and the previously generated ground truth data as the metric. Each cell holds probability values $\mathbf{m} = (m_e, m_o, m_u)$ corresponding to the three states, Empty, Occupy, and Unknown, and we assume that these values are stored in each cell. Among these three probabilities, let the largest one be denoted by $p_{\max}$ and the sum of the remaining two be denoted by p_{others}.

When the following condition is satisfied, $p_{\max} - p_{\text{others}} \geq \theta$, the cell is judged to be in the state corresponding to $p_{\max}$. Here, θ is a threshold value, which is set to $\theta = 0.8$ in this study. The resulting decisions are compared with the ground truth data for each cell, and the ratio of the number of cells that match the ground truth to the total number of cells is used as the accuracy.

As mentioned in the previous subsection, processing time is compared among the three methods, Conventional, Baseline, and proposed, whereas for accuracy we compare only Baseline and proposed and exclude Conventional from the comparison.

D. Comparison Results of Processing Time

For the comparison of processing time, we used the three methods, Conventional, Baseline, and proposed. Each method was executed 30 times, and the average processing time is shown in Table II.

From the measurement results, we observe that Conventional has the largest processing time, while Baseline and proposed are significantly faster. Comparing Baseline and proposed, the difference is about 10 seconds, with Baseline being faster.

This difference is considered to be due to the computational complexity of each method. As described in Section III, the proposed method uses the distance weighted Dempster's rule of combination that takes into account the distance between sensors and grid cells, whereas Baseline uses the standard Dempster's rule of combination. Therefore, the computational cost per fusion operation is higher in the proposed method than in Baseline. Although the difference for each individual fusion operation is small, it is applied repeatedly to all grid cells, which results in an overall processing time difference of about 10 seconds. It should be noted that the processing times reported here correspond to the total runtime of the offline simulation and do not directly represent the end-to-end latency of a real-time V2X system. In practical deployments, feasibility should be evaluated in terms of per-update latency under a target update rate, and the proposed method can be accelerated through parallel processing across grid cells and sensors.

TABLE I: Parameter settings for comparison methods.

Item	Conventional	Baseline	Proposed
Number of sensors	40	16	16
Sensor allocation	Random	Fixed	Fixed
Number of detected grids	Irregular	All cells in area	All cells in area
Number of sensor-fusion per grid	Irregular	4	4
Sensor fusion method	Standard Dempster combination	Standard Dempster combination	Distance-weighted Dempster combination

TABLE II: Processing time.

	Conventional	Baseline	Proposed
processing time [s]	271.2	154.1	166.7

TABLE III: Accuracy experiment: number of grids not exceeding the threshold.

Method \ γ	6	8	10	12	14
Proposed	1,425	3,971	27,462	129,740	336,247
Baseline	4,728	59,862	252,652	536,355	710,003

E. Comparison Results of Accuracy

In the accuracy evaluation, we compare Baseline and the proposed method based on the thresholding rule defined in the previous subsection. First, Table III summarizes the number of grid cells that did not exceed the threshold. The number of grids that did not exceed the threshold in each column represents the number of cells whose probability vector does not exceed the threshold θ in any component, i.e., cells for which a confident decision could not be made. Therefore, smaller values can be interpreted as higher accuracy. From the table, we observe that for all values of the false-detection-rate parameter, the proposed method yields far fewer below-threshold grid cells than Baseline and thus achieves higher accuracy.

Fig. 2 shows the accuracy as a function of the distance-dependent error growth coefficient γ. The vertical axis indicates the proportion of grid cells whose estimated state matches the ground truth, and the horizontal axis indicates the false-detection-rate parameter. The figure shows that, under easy sensing conditions (small horizontal-axis values), the difference between the two methods is relatively small, whereas as the conditions become more difficult, the agreement rate of Baseline drops sharply while the proposed method maintains a high agreement rate. Especially for larger parameter values, the proposed method significantly outperforms Baseline, indicating that the distance-aware hybrid combination rule is effective in improving detection performance under adverse conditions.

Overall, Baseline has a slight advantage in terms of processing time, whereas the proposed method shows a clear advantage in terms of accuracy. Given the modest increase in processing time (about 10 seconds) and the larger accuracy gains in challenging environments, Proposed achieves higher accuracy than Baseline with only a small additional runtime in our experiments.

V. Discussion

In this section, based on the results obtained in Section IV, we discuss how the proposed method can contribute to improving traffic safety at intersections, as outlined in Section I. We also describe the limitations of this study and directions for future work.

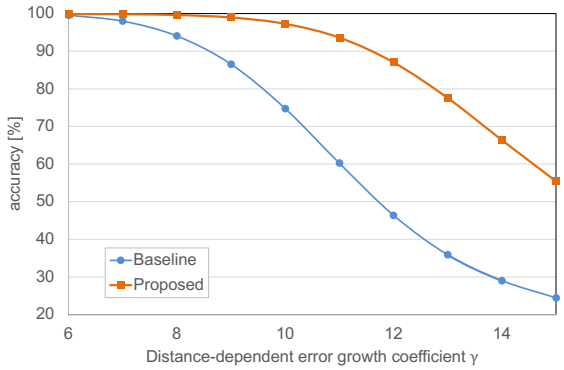

Fig. 2: Accuracy comparison of fusion methods: the standard Dempster's rule of combination is used as the baseline under a shared occupancy-grid representation with an explicit Unknown state, and is compared with its distance-weighted extension.

A. Implications for Traffic Safety at Intersections

In the V2X-based cooperative perception system considered in this paper, multiple sensors and roadside units (RSUs) deployed around an intersection cooperate to provide surrounding environment information to vehicles via an occupancy grid map. From the results in Section IV, it was shown that, compared with the Baseline, Proposed can significantly reduce the number of grid cells that do not exceed the confidence threshold, especially for cells located far from the sensors. This means that the states Occupy/Empty can be determined with higher confidence even for pedestrians and vehicles located in poorly visible areas or deep inside the intersection.

Many serious accidents at intersections are related to collision risks arising from driver blind spots or delayed recognition, such as collisions between right-turning vehicles and oncoming through traffic, or between left-turning vehicles and crossing pedestrians. If a more accurate occupancy grid map is obtained by Proposed, the risk estimation modules in RSUs and vehicles can detect and predict potentially dangerous objects inside the intersection, even when they are outside the field of view of human drivers or automated driving systems, at an earlier stage. For example, when the Occupy probability of a specific grid cell in the intersection (such as a crosswalk or the conflict area with a right-turn lane) exceeds a certain threshold, prompting deceleration or issuing a warning at that moment could reduce collision risk in advance.

Furthermore, it was shown that Proposed maintains a higher agreement rate than the Baseline even when sensing conditions deteriorate. In situations with low visibility, such as dense fog, heavy rain, or nighttime, ensuring safety using only on-board vehicle sensors becomes difficult; however, by complementing information from distant and occluded regions through distance-weighted sensor fusion, Proposed is expected to help improve safety at intersections under such adverse conditions.

B. Limitations and Future Work

On the other hand, this study has several limitations. First, the evaluation in this paper is based on simulations of static occupancy grid maps and does not explicitly model the motion of vehicles and pedestrians (e.g., their speed or acceleration). From the viewpoint of practical traffic-safety assessment, it is necessary to combine not only occupancy states but also dynamic metrics such as Time-To-Collision (TTC) [19] and Post-Encroachment Time (PET) [20].

Second, in this study we simplified sensor characteristics and modeled homogeneous sensors as having identical performance. In real intersections, however, heterogeneous sensors with different properties coexist, including in-vehicle cameras, LiDAR, radar, and roadside cameras. To extend Prop to such environments, we need a more general weighting design that incorporates not only distance but also factors such as sensor type, field of view, and detection latency.

Third, this study does not take into account the effects of communication delay or packet loss. In V2X environments, the communication quality between RSUs and vehicles directly affects the freshness of the occupancy grid map, and therefore an important direction for future work is to investigate real-time implementations that balance the computational cost of Proposed with communication latency.

VI. Conclusion

We proposed a distance-weighted Dempster's rule for V2X cooperative perception at intersections, accounting for sensor-to-cell distance. Compared with standard Dempster fusion, it improved agreement with ground truth, especially for far cells and degraded sensing, while only slightly increasing processing time.

As future work, we plan to integrate the proposed method with traffic flow simulators and real vehicle experiments, and quantitatively evaluate how cooperative perception based on the proposed fusion can reduce near miss events at intersections and improve time to collision margins.

Acknowledgment

These research results were obtained from the commissioned research(No.24101) by National Institute of Information and Communications Technology (NICT), Japan.

References

[1] V. A. Adewopo, N. Elsayed, Z. ElSayed, M. Ozer, A. Abdelgawad, and M. Bayoumi, "A Review on Action Recognition for Accident Detection in Smart City Transportation Systems," *Journal of Electrical Systems and Information Technology*, vol. 10, no. 57, 2023.

[2] H. B. Pasandi and T. Nadeem, "CONVINCE: Collaborative Cross-Camera Video Analytics at the Edge," in *Proceedings of the IEEE International Conference on Pervasive Computing and Communications Workshops (PerCom Workshops)*, 2020, pp. 1–5.

[3] W. Zimmer, G. A. Wardana, S. Sritharan, X. Zhou, R. Song, and A. C. Knoll, "TUMTraf V2X Cooperative Perception Dataset," in *Proceedings of the IEEE/CVF Conference on Computer Vision and Pattern Recognition (CVPR)*, 2024, pp. 22 668–22 677.

[4] S. Miyata and T. Miyata, "Accuracy based rewarding for sensors in noisy collaborative point cloud acquisition environments," in *2025 International Conference on Artificial Intelligence in Information and Communication (ICAIIC)*, 2025, pp. 0402–0407.

[5] A. P. Dempster, "A generalization of bayesian inference," *Journal of the Royal Statistical Society: Series B (Methodological)*, vol. 30, no. 2, pp. 205–232, 1968.

[6] G. Shafer, *A Mathematical Theory of Evidence*. Princeton University Press, 1976.

[7] R. C. Luo, C.-C. Yih, and K. L. Su, "Multisensor fusion and integration: approaches, applications, and future research directions," *IEEE Sensors journal*, vol. 2, no. 2, pp. 107–119, 2002.

[8] D. L. Hall and S. A. McMullen, *Mathematical techniques in multisensor data fusion*. Artech House, 2004.

[9] S. Gao, Y. Zhong, and W. Li, "Random weighting method for multisensor data fusion," *IEEE Sensors Journal*, vol. 11, no. 9, pp. 1955–1961, 2011.

[10] A. A. Bardwaj, M. Anandaraj, K. Kapil, S. Vasuhi, and V. Vaidehi, "Multi sensor data fusion methods using sensor data compression and estimated weights," in *2008 International Conference on Signal Processing, Communications and Networking*, 2008, pp. 250–254.

[11] S. Ishihara and M. Yamakita, "Gain constrained robust ukf for nonlinear systems with parameter uncertainties," in *2016 European Control Conference (ECC)*, 2016, pp. 1709–1714.

[12] J. K. Wu and Y. F. Wong, "Bayesian approach for data fusion in sensor networks," in *2006 9th International Conference on Information Fusion*, 2006, pp. 1–5.

[13] Q. Zhang, L. Sun, and Y. Jin, "Description of key performance index states based on cloud theory and weight mean method for multi-sensor," in *Eighth ACIS International Conference on Software Engineering, Artificial Intelligence, Networking, and Parallel/Distributed Computing (SNPD 2007)*, vol. 1, 2007, pp. 350–354.

[14] Z. Ying, L. Hongsheng, and D. Yongzhong, "Self-adaptive sensor weighted data fusion in strain detection," in *2007 8th International Conference on Electronic Measurement and Instruments*, 2007, pp. 4–55–4–58.

[15] J. Zhang, K. Wang, and Q. Yue, "Data fusion algorithm based on functional link artificial neural networks," in *2006 6th World Congress on Intelligent Control and Automation*, vol. 1, 2006, pp. 2806–2810.

[16] S. Yamada, Y. Watanabe, and H. Takada, "Distributed environmental information management system for autonomous vehicles using edge computing (in Japanese)," *Journal of the Robotics Society of Japan*, vol. 38, pp. 199–209, 01 2020.

[17] F. Camarda, F. Davoine, and V. Cherfaoui, "Fusion of evidential occupancy grids for cooperative perception," in *Proceedings of the Annual Conference on System of Systems Engineering*, 2018, pp. 284–290.

[18] S. Ben Ayed, J. Dachraoui, and H. Laghmara, "Overview on evidential fusion approaches in the context of collaborative perception for occupancy modeling," *Appl Intell*, vol. 55, no. 822, 2025.

[19] J. C. Hayward, "Near-miss determination through use of a scale of danger," *Highway Research Record*, 1972. [Online]. Available: https://api.semanticscholar.org/CorpusID:53468218

[20] B. L. Allen, B. T. Shin, and P. J. Cooper, "Analysis of traffic conflicts and collisions," *Transportation Research Record*, 1978. [Online]. Available: https://api.semanticscholar.org/CorpusID:92979323